UNIVERSITÀ POLITECNICA DELLE MARCHE
Repository ISTITUZIONALE

Influence of a lipophilic edaravone on physical state and activity of antioxidant liposomes: An experimental and in silico study

This is the peer reviewd version of the followng article:

Original
Influence of a lipophilic edaravone on physical state and activity of antioxidant liposomes: An experimental and in silico study / Minnelli, C.; Laudadio, E.; Fiorini, R.; Galeazzi, R.; Armeni, T.; Stipa, P.; Rusciano, D.; Mobbili, G.. - In: COLLOIDS AND SURFACES. B, BIOINTERFACES. - ISSN 0927-7765. - STAMPA. - 210:(2022). [10.1016/j.colsurfb.2021.112217]

Availability:
This version is available at: 11566/293789 since: 2024-04-09T15:14:53Z

Publisher:

Published
DOI:10.1016/j.colsurfb.2021.112217

Terms of use:

The terms and conditions for the reuse of this version of the manuscript are specified in the publishing policy. The use of copyrighted works requires the consent of the rights' holder (author or publisher). Works made available under a Creative Commons license or a Publisher's custom-made license can be used according to the terms and conditions contained therein. See editor's website for further information and terms and conditions.
This item was downloaded from IRIS Università Politecnica delle Marche (https://iris.univpm.it). When citing, please refer to the published version.

(Article begins on next page)

23 November 2024

Influence of a lipophilic Edaravone on physical state and activity of antioxidant liposomes: an experimental and *in silico* study

Cristina Minnelli[1], Emiliano Laudadio[2], Rosamaria Fiorini[1], Roberta Galeazzi[1], Tatiana Armeni[3], Pierluigi Stipa[2], Dario Rusciano[4], Giovanna Mobbili[1]*

1 Dipartimento di Scienze della Vita e dell'Ambiente (DISVA), Università Politecnica delle Marche, via Brecce Bianche, 60131 Ancona, Italy
2 Dipartimento di Scienze e Ingegneria della Materia, dell'Ambiente e Urbanistica (SIMAU), Università Politecnica delle Marche, via Brecce Bianche, 60131 Ancona, Italy
3 Dipartimento Scienze Cliniche Specialistiche ed Odontostomatologiche, Università Politecnica delle Marche, via Brecce Bianche, 60131 Ancona, Italy
4 Sooft Italy SpA, 95100 Catania, Italy

*Correspondence; g.mobbili@staff.univpm.it; +390712204707

Short statistical summary

Number of words: 5998

Number of Figures: 4

Number of Tables: 2

Influence of a lipophilic Edaravone on physical state and activity of antioxidant liposomes: an experimental and *in silico* study

Cristina Minnelli[1], Emiliano Laudadio[2], Rosamaria Fiorini[1], Roberta Galeazzi[1], Tatiana Armeni[3], Pierluigi Stipa[2], Dario Rusciano[4], Giovanna Mobbili[1]*

1 Dipartimento di Scienze della Vita e dell'Ambiente (DISVA), Università Politecnica delle Marche, via Brecce Bianche, 60131 Ancona, Italy
2 Dipartimento di Scienze e Ingegneria della Materia, dell'Ambiente e Urbanistica (SIMAU), Università Politecnica delle Marche, via Brecce Bianche, 60131 Ancona, Italy
3 Dipartimento Scienze Cliniche Specialistiche ed Odontostomatologiche, Università Politecnica delle Marche, via Brecce Bianche, 60131 Ancona, Italy
4 Sooft Italy SpA, 95100 Catania, Italy

*Correspondence; g.mobbili@staff.univpm.it; +390712204707

Abstract

The influence of a lipophilic derivative of Edaravone (C18Edv) on a POPC liposomal bilayer has been investigated by a combined computational-experimental approach. The order and hydration degree of three different systems composed by 10%, 20% and 40% in w/w percentage of C18Edv respect to POPC were investigated through Molecular Dynamics (MD) simulations and fluorescence spectroscopy experiments. Dynamic Light Scattering measurements showed how the presence of different amounts of C18EdV determines differences on liposome size and stability. The survey revealed that the content of lipophilic antioxidant tunes liposome rigidity and influences cellular uptake and antioxidant activity which are maximized for formulation containing 20% of C18Edv.

Keywords: antioxidant liposomes; lipophilic Edaravone; Dynamic Light Scattering; fluorescence spectroscopy; MD simulations

1. Introduction

Antioxidant liposomes are bilayer vesicles containing antioxidant enzymes, lipophilic molecules or water-soluble chemical antioxidants. They can play a prominent role in the treatment of many diseases in which the body is not able to prevent a pathologic oxidative stress. Lipid membranes, proteins and DNA can be the target of free radical's attack and their damage is responsible of neurodegenerative disorders, atherosclerosis, cardiac ischemia reperfusion injury and cancer [1,2]. In this background, Edaravone (Edv) is a neuroprotective agent known for its potent antioxidant protection against oxidative stress and neuronal apoptosis [3]. In the context of a research on membrane-targeting antioxidants more efficient in preventing lipid peroxidation (LPO), we recently synthesized 3-methyl-4-octadecyl-1-phenyl-2-pyrazolin-5-one (C18Edv), a lipophilic derivative of Edv possessing a fully saturated C18 hydrocarbon chain at C-4 in the pyrazolone ring (Figure 1A) [4]. The increased affinity of C18Edv toward the lipid membrane allowed to obtain a greater protective efficacy on the oxidative stress-induced cell death [4]. Such a lipophilic molecule needs to be encapsulate into a vector in order to overcome its poorly water solubility; in the broad panorama of nanoparticles, liposomes represent versatile and biocompatible platforms that can be easily prepared with tunable properties to incorporate both hydrophilic and lipophilic drugs. It is important to consider that the incorporation of any guest molecule can potentially affect vector physicochemical parameters and drug delivery performance that dramatically depends on properties such as liposome

size, z-potential, fluidity, and stability. The aim of this study is to investigate by a combined computational-experimental approach how the presence of C18Edv modifies a POPC liposomal bilayer. In the *in-silico* investigation three different systems composed by 10%, 20% and 40% in w/w percentage between C18Edv and POPC were then generated, and the order and hydration degree were investigated through Molecular Dynamics (MD) simulations. Because membrane physical state can affect liposome ability to deliver a bioactive molecule, POPC liposomes containing the same percentage of C18Edv employed in the computational studies were prepared and investigated by fluorescence spectroscopy and cellular experiments. Two different types of fluorescent probes were employed: DPH, which partitioned deep in the hydrophobic interior of the liposome, and Laurdan, which partitioned at the surface of the bilayer. Both MD and fluorescence results suggested that C18Edv tunes the liposome rigidity and hydration. The presence of different amounts of C18EdV determines differences on liposome size and stability. The survey was compared with the ability of liposomes containing C18Edv to be internalized and to act as antioxidant liposomes in contrasting AAPH-induced cell death in adult retinal pigmented epithelium (ARPE-19) cells.

2. Materials and methods

2.1. Materials

1-palmitoyl-2-oleoyl-sn-glycero-3-phosphocholine (POPC), 2,2-azobis (2-amidinopropane hydrochloride) (AAPH), 1,6-Diphenyl-1,3,5-hexatriene (DPH), 6-dodecanoyl-2-dimethylamine-naphthalene (Laurdan), sephadex G-50, 3-(4,5-dimethylthiazol-2-yl-2,5-diphenyl tetrazolium bromide (MTT), hydrogen peroxide and all solvents were obtained from Merck (Stenheim, Germany). 3-methyl-4-octadecyl-1-(pyridin-2-yl)-5-pyrazolone (C18Edv) has been synthesized as previously described [4]. All the solutions were prepared in ultrapure MilliQ water. Adult human retinal pigment epithelial (ARPE-19) cells (CRL 2302) were obtained from American Type Culture Collection (ATCC) Manassas, Virginia, USA. All cell culture reagents were purchased from Euroclone (Euroclone, Italy).

2.2. Molecular Dynamics Simulations

A membrane bilayer system consisting of 128 POPC (1-palmitoyl-2-oleoylphosphatidylcholine) fully hydrated lipids was built using Charmm GUI membrane builder tool [5] to simulate a section of empty liposome (Lips). The model was minimized and then equilibrated by a preliminary NPT MD simulation. Different numbers of C18Edv molecules were added randomly substituting pre-equilibrated POPC lipids to reproduce the labelling percentage of samples used for experimental approach. Three different models were then generated, with POPC and 10%, 20% and 40% of C18Edv concentration. The overall box dimensions were 6.62 nm × 6.62 nm × 8.5 nm, in line with literature, concerning the smallest representative size that can be used to accurately reproduce the occurring intermolecular interactions in lipid bilayers [6][7]. The simulation model systems were appropriately solvated and water−water interactions were modelled by using TIP3P model [8] whereas hydrogen bonds within the solvent molecules were constrained using the SHAKE algorithm [9]. GROMACS 5.0.4 suite of programs [10] was used to perform all MD simulations, using AMBER99SB force field [11], and extending its parameterization to provide the accurate description of C18Edv molecules. New atom types were then included, using B3LYP/6-311G** at the density functional theory (DFT) level [12][13][14] and included in the force field parameters [15]. The bilayer energy was minimized applying periodic box conditions in all directions, using a neighbour searching grid type; the cut-off distance for the short-range neighbour list was set to 1.4 nm. Electrostatic

interactions were taken into account by implementing a fast smooth particle-mesh Ewald algorithm [16][17] with a 1.4 nm distance for the Coulomb cut-off because this method is considered to be both efficient and accurate for the evaluation of long-range electrostatic interactions in large macromolecular systems [18].
After a massive minimization, the Lips-C18Edv-10%, Lips-C18Edv-20% and Lips-C18Edv-40% systems underwent to a preliminary equilibration based on 2 ns of annealing simulations. A weak temperature coupling (Berendsen thermostat), with a time constant of 1 ps, was applied to maintain the reference temperature (310 K) throughout the whole run. The subsequent production step consisted in 100 ns of MD simulation in isothermal−isobaric (NPT) ensemble at 1 atm and 310 K (37°C) for all equilibrated systems [19]. A time constant for coupling of 0.5 ps and an optimal compressibility for water of $4.5 \times 10{-}5$ bar^{-1} were used to obtain the best control on pressure. The achievement of a steady state for all of the simulated models was monitored through the molecular root-mean-square deviation (rmsd) values versus time [20]. Deviation was calculated as displacement with respect to the starting minimized structure. The analysis of the simulations' trajectories was performed by means of the VMD [21] and CHIMERA software [22]. The deuterium order parameter (S_{cd}) profiles as a function of the carbon atom number of CH_2 groups for the two acyl chain types (palmitic and oleic) of the POPC molecules have been calculated from MD trajectories. This analysis represents commonly used measure to characterize the order in the lipid bilayers, and then, the fluidity degree. A higher order degree is related to a lower membrane fluidity. The S_{cd} was calculated using the equation:

$$S_{cd} = \frac{1}{2}(3\cos^2\theta_i - 1)$$

where θ_i is the angle between the molecular axis given by the carbon atoms C_{i-1} and C_{i+1} and the lipid bilayer normal axis.
The hydration degree of the POPC polar headgroups has been evaluated monitoring the hydrogen bond interactions between lipids and water molecules. Two groups for analysis have been generated, the first was related to the polar parts of all POPC lipids, while the second one was related to all water molecules. All hydrogen bonds between the two groups have been analysed, then the average hydration degree (H_d) of POPC molecules in the four different systems has been extrapolated using the equation:

$$H_d = \frac{N_{HB}}{N_{PH}}$$

In which N_{HB} is the total number of H bonds between water molecules and POPC lipids, and N_{PH} represents the total number of the polar headgropus of POPC lipids.

2.3. Liposome preparation

Liposomes containing C18Edv were prepared by "thin film hydration" method. Appropriate amounts of chloroform solutions of POPC and methanol solutions of C18Edv (10, 20 and 40% w/w of C18Edv with respect to phospholipid) were mixed; after removing the solvent by evaporation under reduced pressure, the film was dried under vacuum for 4 h and then resuspended in the required amount of sterile PBS (pH 7.4) to obtain Lips-C18Edv-10%, Lips-C18Edv-20% and Lips-C18Edv-40%. The final concentration of POPC was 3mM. Empty liposomes were also prepared as control. The resulting multilamellar vesicle dispersions were sonicated (10 min, 50%) with a vibra cell sonicator (Sonics Vibra Cell Mod. VCx130) equipped with a tapered micro tip.

2.4. Fluorescence Spectroscopy Measurements

The fluorescence measurements have been performed at 37°C with a computer-controlled PerkinElmer LS55 spectrofluorimeter. The temperature was measured in the sample by a digital thermometer. The background fluorescence of the samples was checked prior to each measurement, and was negligible when the probes were added. Stock solutions of Laurdan (6-dodecanoyl-2-dimethylamine-naphthalene) in ethanol and DPH (1,6-diphenyl-1,3,5-hexatriene) in tetrahydrofuran were added to liposomal suspensions (0.3 mM POPC concentration) at final probes concentration of 1 μM; each suspension was incubated in the dark, at 37 °C for 2 h prior to use. Each spectrum corresponds to the average of determinations performed on three different samples.
Laurdan spectral changes have been used to calculate the generalized polarization (GP), a function which gives information about the lipid packing related to the water content and dynamics at the lipid interface [23]. Laurdan excitation GP (Ex GP) and emission (Em GP) spectra have been calculated as follow [24]:

$$\text{Ex GP}=(I_{440}-I_{490})/(I_{440}+I_{490})$$

where I_{440} and I_{490} are the intensities at each excitation wavelength, from 320 to 420 nm, obtained using a fixed emission wavelength of 440 and 490 nm, respectively.

$$\text{Em GP}=(I_{390}-I_{360})/(I_{390}+I_{360})$$

where I_{390} and I_{360} are the intensities at each emission wavelength, from 420 to 550 nm, obtained using a fixed excitation wavelength of 390 and 360 nm, respectively.

For the DPH-labelled liposomes, the fluorescence anisotropy was calculated by using the following equation:

$$r_s = (I_{\parallel} - I_{\perp} xg)/(I_{\parallel} + 2I_{\perp} xg)$$

where g is an instrumental correction factor, $I_{\parallel}$ and $I_{\perp}$ are, respectively, the emission intensities with the polarizers parallel and perpendicular to the direction of the polarized exciting light.

2.5. Dynamic Light Scattering (DLS) characterization

The intensity-based diameter (Z-average) and the zeta potential of all formulations were measured by Dynamic Light Scattering (DLS) and Electrophoretic Light Scattering using a Malvern Zetasizer Nano ZS (Malvern Instruments GmbH). An aliquot of every liposome suspension was diluted at a final concentration of $3x10^{-2}$ mM with ultra-purified water and analysed after 24 h and 1 month of preparation. The colloidal stability of all systems was also studied in physiological conditions by mixing the samples with DMEM medium supplemented with Fetal Bovine Serum (FBS) (10% v/v) to reach a final concentration of 3×10^{-2} mM and the analyses performed immediately after liposomes preparation and after 24 h. Measurements were performed at 25 °C with a fixed angle of 173°. Size particle polydispersity index were calculated from the autocorrelation function by cumulant analysis (Dispersion Technology Software V7.11 provided by Malvern Instruments). Zeta potentials were determined by the Zetasizer software from the electrophoretic mobility applying Henry's equation

and using Smoluchowski's approximation. For all samples investigated, the data represent the average of at least three different autocorrelations carried out for each sample.

2.6. Determination of Encapsulation Efficiency by gel filtration method

Liposomal formulations, containing increasing C18Edv concentrations, were purified from the free antioxidants by size exclusion chromatography. Empty liposomes and free C18Edv were also used as control. The encapsulation efficiency was determined on the collected eluates by lysing purified and unpurified liposomes: 0.5 mL samples were added to 1% Triton X-100 (v/v) and the antioxidants concentration was estimated by the Folin-Ciocalteu assay [4]. 0.15 mL of 30% Folin-Ciocalteu reagent was added to 0.05 mL of every sample into a 96-well microplate and shaken. After 10 min 0.1 mL of a 7.5% sodium carbonate solution was added and the mixtures were incubated in the dark for 1 h at room temperature for color development. After incubation, the absorbance was measured at 765 nm on a BioTek Synergy HT MicroPlate Reader Spectrophotometer using a blank containing all the appropriate components except C18Edv. The calibration curve was plotted using C18Edv solutions in PBS with 1% Triton X-100 (v/v). The Encapsulation Efficiency (EE) was determined using following formulas:

$$EE\ (\%) = 100 \times [(C_{int})/ C_{total}]$$

where the C_{total} refers to the total concentration of antioxidant measured in the not filtered dispersions, C_{int} refers to the concentration of the encapsulated molecule (which was the amount of antioxidant measured inside purified liposomes. All the experiments were repeated at least three times and measurements were run in triplicate.

2.7. Cellular Experiments

2.7.1. Protection Assay

For treatments, ARPE19 cells were seeded in 24-well plates at $8x10^4$/well to reach 60% of confluence after 24 h. Then, the medium from each well was replaced with fresh medium containing empty liposomes (Lips) and liposomes formulations prepared at 10% and 20% (w/w, antioxidants/lipid) (Lips-C18Edv-10%, Lips-C18Edv-20%). The results were compared with the equal concentration of free C18Edv in methanol (0.1 mM). After incubation for 24 h, cells were washed twice with PBS and treated with AAPH (15 mM) for additional 24 h. Previous cellular viability assays were performed in order to establish the combination of dose/time of AAPH able to induce 50% of cell death after 24 h of treatment, cytotoxicity of empty liposomes (data not shown) and the cytotoxicity of free C18Edv [4]. Number of viable cells, and thus the protection from oxidative stress induced cell death, was estimated by 3-(4,5-dimethylthiazol-2-yl)-2,5-diphenyltetrazolium bromide (MTT) assay. At the time of analyses, the medium from each well was removed and replaced with fresh medium supplemented with MTT at a final concentration of 0.1 mg mL, and the cells incubated for 3 h at 37 °C in 5% CO_2 atmosphere. Then 0.4 mL of DMSO was used to solubilize the purple formazan crystals formed from MTT reduction. The absorbance was read on a multiwell scanning microplate reader (BioTek Synergy HT MicroPlate Reader Spectrophotometer, BioTek Instruments Inc., Winooski, VT, USA) at 570 nm using the extraction buffer as a blank. The optical density in the control group (untreated cells) was considered as 100% viability. The relative cell viability (%) was calculated as (A570 of treated samples/A570 of untreated samples) x 100. Determinations were carried out in triplicate in each experiment and mean ± SD from five independent experiments was calculated.

2.7.2. Liposomal uptake study

To estimate the intracellular uptake of Lips-C18Edv-10%, Lips-C18Edv-20% formulations, the molecular probe calcein was used as previously described [25]. ARPE19 cells were plated on a 6-

well plate to achieve 70% confluence after 24 h of treatment. After that, complete culture medium was replaced with serum free DMEM/F12 containing Lips-C18Edv-10% and Lips-C18Edv-20% at final lipid concentration of 90 µg mL. After 4 h of incubation, cells were washed three times with PBS and the liposome uptake was assessed by flow cytometric analysis.
The fluorescence of calcein free- and liposome-treated cells was measured in a Beckman Coulter Epics XL cytometer (Beckman Coulter, Miami, FL) using an excitation wavelength of 517 nm and the mean fluorescence intensity of calcein was quantified using FlowJo® software (FlowJo LLC, Ashland, OR, USA).

3. Results and Discussion

3.1. Effect of C18Edv encapsulation on the liposome membrane properties

3.1.1. Molecular Dynamics Investigations

Representative models of POPC liposomes (Lips) containing increasing C18Edv concentrations (Lips-C18Edv-10%, Lips-C18Edv-20% and Lips-C18Edv-40%) are shown in **Figure 1B-D**. Investigating root mean square deviations (RMSD) (**Figure 1E**), it can be noticed that after an initial fluctuation, all atoms in the simulated systems reached a stable positioning; in particular, all the curves reached to a stable plateau after 40 ns, remarking the achievement of very stable systems regardless the presence of C18Edv inside the membrane.

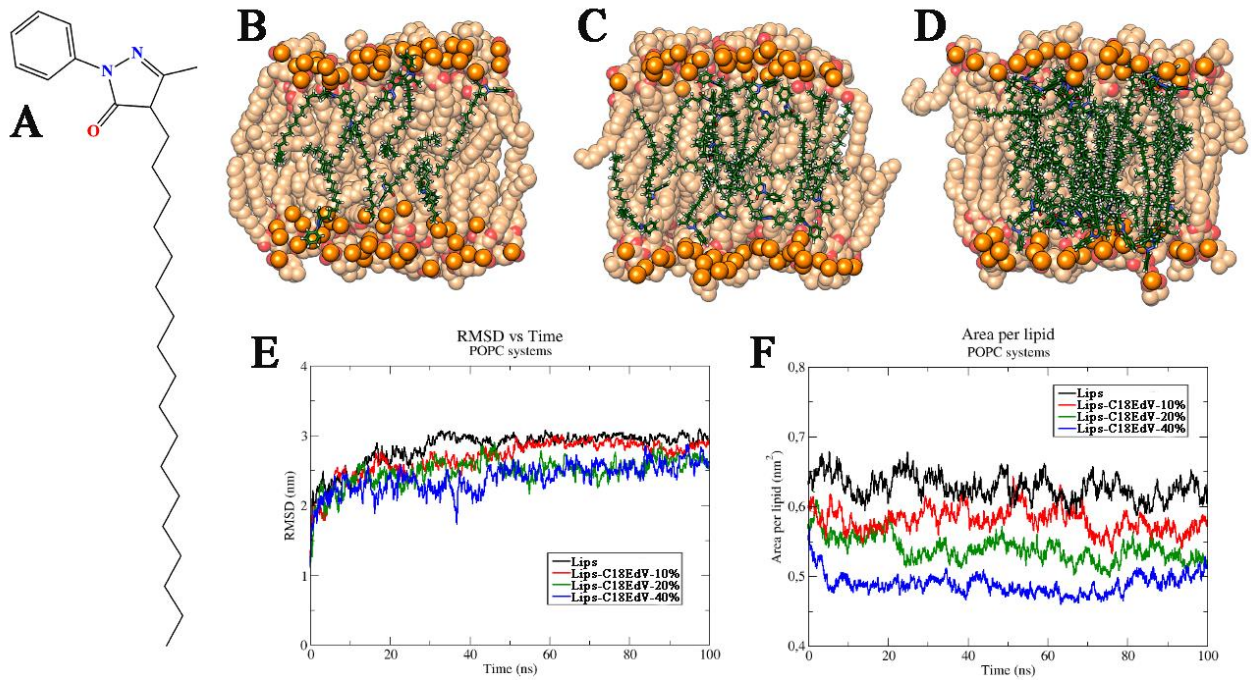

Figure 1. Molecular structure of C18Edv (**A**). Snapshots of Lips-C18Edv-10% **(B),** Lips-C18Edv-20% **(C)** and Lips-C18Edv-40% **(D).** The phosphorus atoms and the POPC molecules are reported in orange and yellow VdW spheres, respectively. C18Edv molecules are reported in green. The root-mean-square deviation of POPC lipids in the four investigated systems **(E)**. Area per lipid as a function of time for the four investigated systems **(F)**.

When the membrane is composed by different types of phospholipids, neighbouring interactions between the lipids can lead to a change in the membrane parameters, as average cross-section *area per lipid*. A_{mol} in function of MD time has been estimated for each system (**Figure 1F**) by dividing the xy area of MD box by the lipid number in the bilayer leaflet. The plots showed that all molecular areas are sufficiently equilibrated after 60 ns. The estimated A_{mol} of pure POPC bilayer was 0.64 nm^2, comparable with experimental values [26] and decreased when the C18Edv concentration was increased, leading to values of 0.59 nm^2, 0.56 nm^2, and 0.52 nm^2 for Lips-C18Edv-10%, Lips-

C18Edv-20%, and Lips-C18Edv-40% systems respectively. These changes are related to a gradual increase of rigidity degree of systems because the lipids gradually compact more as the concentration of C18Edv increases.

The degree of hydration of the POPC polar headgroups has also been evaluated monitoring the hydrogen bond interactions between lipids and water molecules at last 20 ns of MD simulations (**Figure 2A**). Hydrogen bonds (HB) have been determined on the base of cut-offs for the angle hydrogen - donor - acceptor and the distance donor – acceptor (**Figure 2B-C**).

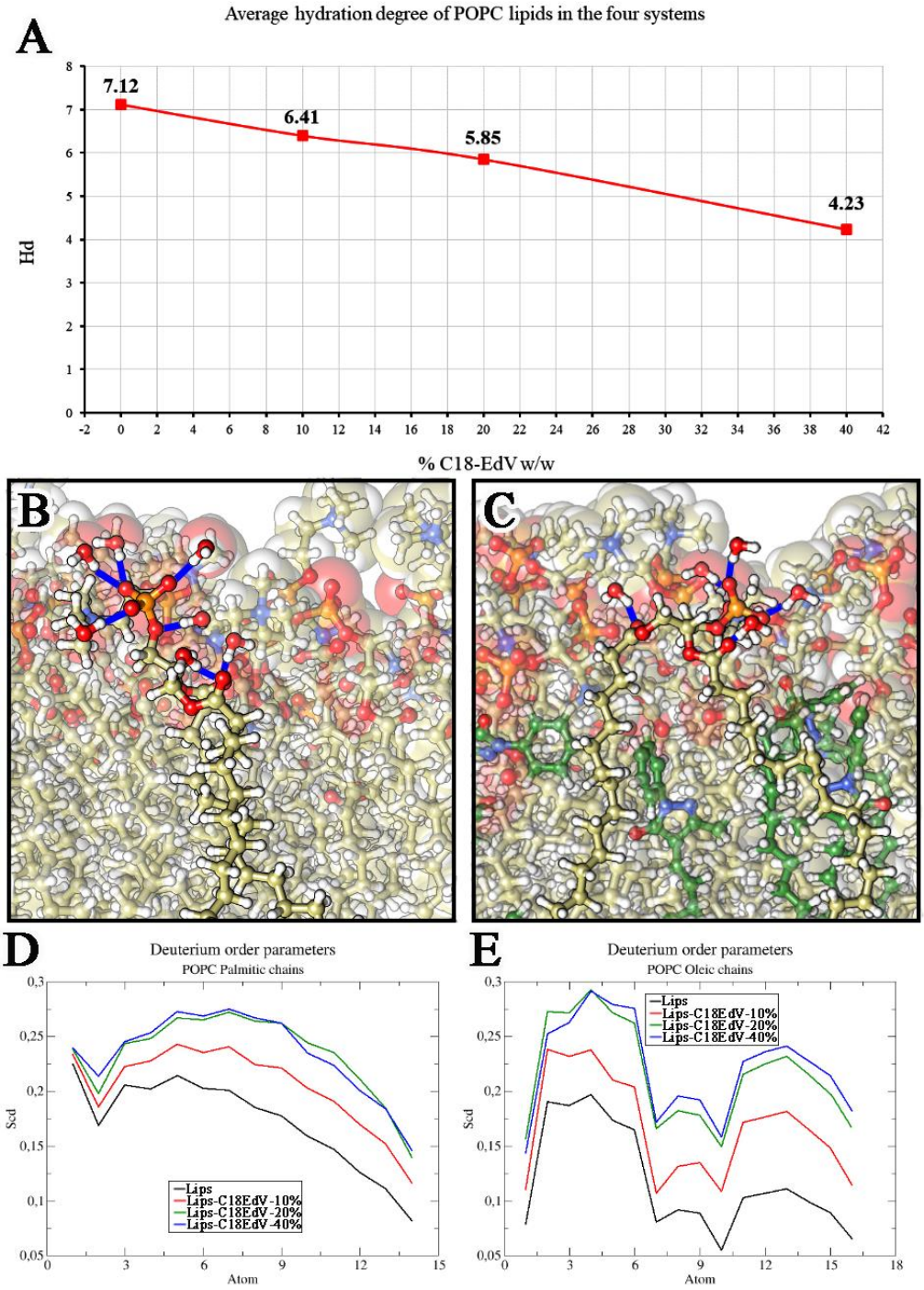

Figure 2. Average Hydration Degree of POPC headgroups at increasing C18Edv concentrations (0, 10%, 20%, and 40%) **(A).** Water-POPC hydrogen bonds (HB) interactions in Lips **(B)** and Lips-C18Edv-20% **(C).** The HBs are reported in thick blue lines. Deuterium order parameters of Palmitic **(D)** and Oleic **(E)** chains of POPC lipids. Lips, Lips-C18Edv-10%, Lips-C18Edv-20%, and Lips-C18Edv-40% are reported in black, red, green, and blue, respectively.

The POPC pure system showed a H_d value of 7.12, meaning that a lot of water molecules are able to penetrate the polar portions of POPC lipids to generate a lot of HBs. Adding 10% of C18Edv, the H_d value decreased to 6.41; the decrease of the number of water molecules close to the polar portions is due to an increase in the rigidity of the polar headgroups of lipid system. In the Lips-C18Edv-20%, this effect appeared more evident, because the H_d value was 5.85, and reaching 40% of C18EdV, H_d value became 4.23. The H_d investigation showed that the influence of C18Edv on the POPC system rigidity is directly proportional to the amount of C18Edv present. To provide detailed information regarding the overall order of the membrane, the deuterium order parameter (S_{cd}) has been used to specifically consider the acyl groups and evaluate the rigidity degree of POPC lipid core systems with and without the C18Edv addition. The S_{cd} analysis computes the order parameter per atom for POPC carbon tails. For atom i, the vector i-1, i+1 is used along lipid membrane normal. To focus on the steady states of systems, the profiles of the S_{cd} parameters have been calculated on the last 20 ns of MD simulations (**Figure 2D and 3E**). The incorporation of C18Edv causes small changes in the dynamic movements of the POPC membrane. In fact, the order parameter of both saturated and the unsaturated acyl chains gradually increased passing from POPC pure system, to POPC with 20% w/w C18Edv. In contrast, the presence of 40% w/w of C18Edv did not significantly change the membrane organization respect to the system containing 20% w/w of C18Edv.

3.1.2. Fluorometric Measurements

The effect of C18Edv on the POPC bilayer properties was also studied experimentally by DPH steady-state fluorescence anisotropy and Laurdan emission and excitation spectral shifts, which were evaluated from the generalized polarization measurements. These fluorescent probes are structurally different and can locate at two different positions in the lipid bilayer; therefore, they can give information about the effect of a guest molecule in both the deep hydrophobic core of acyl chain regions (DPH) and the hydrophobic-hydrophilic interface (Laurdan).

The fluorescent anisotropy of the rod-shaped probe DPH is extensively used to monitor the organization and dynamics of the interior regions in membranes [27]. It provides information about membrane fluidity that is a measure of the bilayer resistance to rotational and translational motions of molecules and reflects lipid packing in the bilayer. DPH steady-state fluorescence anisotropy (r_s) in POPC multilamellar liposomes with and without C18Edv are presented in **Table 1**. All antioxidant concentrations induced a significative increase of DPH steady-state fluorescence anisotropy; the rotational diffusion in the membrane, correlated to the degree of molecular packing of lipid fatty acid chains, appears reduced due to an increase of the environment microviscosity. The presence of C18Edv 10%, 20% and 40% determines a decrease of freedom of rotational motion of the DPH due to much more packed phospholipids surrounding it in the core of the membrane. Our data agree with MD simulation showing that in the presence of C18Edv the order degree of the lipid acyl chains increased from POPC liposomes to POPC with 20% w/w C18Edv but does not undergo significant changes when C18Edv concentration is 40 % w/w.

Table 1. DPH steady state fluorescence anisotropy in POPC liposomes in absence and in presence of 10%, 20% and 40% C18Edv (* P<0.05; ** P<0.01).

Formulation (w/w, host/POPC)	**r_s**
Lips	0.080 $\pm$ 0.006
Lips-C18Edv-10%	0.086 + 0.007*
Lips-C18Edv-20%	0.107 + 0.007**
Lips-C18Edv-40%	0.101 + 0.007**

The peculiar structure of Laurdan with the lauric acid tail anchored in the hydrophobic region of the bilayer and its fluorescent moiety located at the level of the glycerol backbone of the membrane [28] allows to obtain information about the polarity and hydration of the interface between lipid bilayers and bulk water. Laurdan has no preferential phase partitioning between ordered and disordered lipid phases, it is not affected by the chemical nature of phospholipid head group and its lateral and transbilayer distribution can be considered uniform [29]. It is sensitive to polarity changes and dynamic properties at the membrane lipid–water interface due to the content and mobility (solvent relaxation) of water molecules surrounding the fluorophore [30]. Since polarity is very different in the gel and in the liquid-crystalline phases of phospholipids, Laurdan has been shown to be highly sensitive to the phase state of the membrane [31]. In the gel phase both ExGP and EmGP spectra are wavelength independent. In the liquid-crystalline phase, Ex GP values decrease with increasing excitation wavelength, while EmGP values increase with increasing emission wavelength [24]. High Em GP and Ex GP values indicate a rigid membrane with a decrease of content and mobility of water molecules during the fluorescence lifetime, respectively. The wavelength dependence for Laurdan excitation (Ex GP) and emission (Em GP) spectra measured at 37°C in POPC liposomes in the absence and in the presence of C18Edv 10%, 20% and 40% (w/w) are reported in **Figure 3A-B**, respectively.

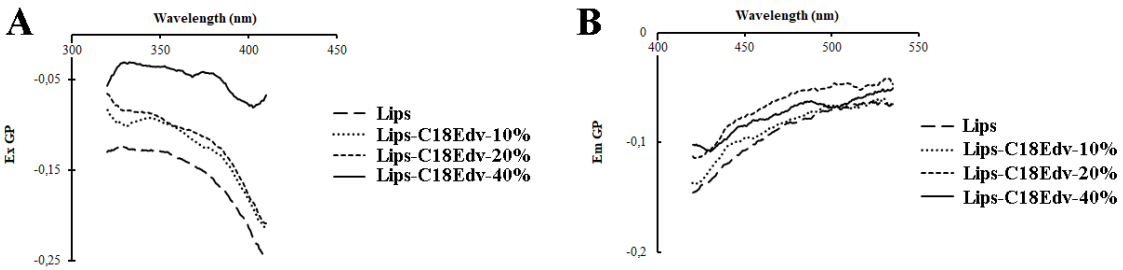

Figure 3. Laurdan excitation **(A)** and emission **(B)** generalized polarization (GP) spectra in POPC liposomes in absence and in presence of 10%, 20% and 40% C18Edv. Each spectrum is the mean ± SD of three different experiments; the SD are not shown for the clarity of the spectra.

We can observe that the fluorescence data obtained for POPC in absence of the guest molecule are characteristic of liquid-crystalline phase. In agreement with Molecular Dynamic simulations, all the concentrations of C18Edv caused a significant increase in Ex GP values, indicating a decrease in the rate of dipolar relaxation of water molecules near the probe due to an increase in Laurdan molecules surrounded by phospholipids much more packed. Moreover, while the guest molecule in C18Edv 10% and 20% did not induce any membrane phase change, the 40% concentration of C18 Edv probably causes a coexistence of gel and liquid-crystalline domains. As presented in **Figure 3A**, C18Edv 10% and C18Edv 20% Laurdan excitation GP spectra show the presence of a homogeneous liquid-crystalline phase with GP values decreasing at longer excitation wavelengths; the Lips-C18Edv-40% Ex GP and EmGP spectra are different and typical of mixed phases with sometimes positive and negative slopes respectively. Changes in the presence and mobility of water dipoles can be evidenced by Laurdan Em GP spectra [30][24]. The results reported in **Figure 3B** show that only C18Edv 20% and 40% were able to increase Em GP values, reflecting a decreased water concentration in the microenvironment probed by Laurdan.

3.2. Dynamic and Electrophoretic Light Scattering

Liposomal formulations containing increasing C18Edv concentrations were characterized for their particles size and zeta potential by Dynamic and Electrophoretic Light Scattering and the results showed in **Table 2**. Empty liposome showed a certain degree of polydispersity (PDI>0.4) with an average diameter of about 100 nm after 24 h of preparation and the size only slight increases after 1 month. The addition of the guest molecule induced an increase in mean diameter in a dose-dependent manner. In particular, the encapsulation of 10% C18Edv did not induce a significative increase in particles size but the polydispersity decreased respect to empty liposomes at all times analysed (PDI=0.25). In the presence of higher C18Edv concentrations, corresponding to 20% and 40% w/w on lipid molecule, the mean diameter increased and both nanoparticles showed a particle size of about 170 nm after 24 h of preparation. After 1 month, a further increase was observed although with different degree. Lips-C18Edv-20% showed a relative colloidal stability and the mean diameter was around 250 nm while for the Lips-C18Edv-40% a few precipitates were observed, the particles size reached 500 nm and the polydispersity was high. This effect could relate to the increase of rigidity showed by DPH steady-state fluorescence anisotropy experiments. The colloidal stability in the culture medium was also evaluated since this is a particularly relevant parameter for use in clinical applications, where nanoparticles are often immersed in whole blood [32][33]. In this condition, both Lips-C18Edv-10% and Lips-C18Edv-20% showed high colloidal stability while in the formulation Lips-C18Edv-40% an increase in mean diameter was observed making this system not suitable for drug delivery application.

Table 2. Properties of Edaravone-C18 Liposomes (Lips-C18Edv)

Formulation (% w/w, host/POPC)	Time of analyses	Mean Diameter in PBS ± SD (nm)	PDI ± SD	ζ-potential ± SD (mV)	Mean Diameter in culture medium ± SD (nm)	PDI ± SD	Encapsulation Efficiency (%)
Lips	0 hrs	118 ± 2	0.41 ± 0.02	- 10 ± 2	109 ± 2	0.42 ± 0.04	-
	24 hrs	109 ± 3	0.43 ± 0.04		122 ± 1	0.43 ± 0.01	
	1 month	135 ± 6	0.53 ± 0.02		-	-	
Lips-C18Edv-10%	0 hrs	104 ± 1	0.25 ± 0.01	- 7 ± 1	89 ± 3	0.21 ± 0.01	99 ± 3
	24 hrs	108 ± 1	0.26 ± 0.04		90 ± 2	0.22 ± 0.01	
	1 month	112 ± 2	0.25 ± 0.01		-	-	
Lips-C18Edv-20%	0 hrs	157 ± 4	0.35 ± 0.02	- 6 ± 1	146 ± 2	0.34 ± 0.3	90 ± 4
	24 hrs	170 ± 1	0.36 ± 0.01		221 ± 3	0.62 ± 0.2	
	1 month	247 ± 2	0.37 ± 0.02		-	-	
Lips-C18Edv-40%	0 hrs	158 ± 2	0.24 ± 0.01	- 6 ± 2	150 ± 2	0.17 ± 0.01	82 ± 8
	24 hrs	169 ± 3	0.22 ± 0.02		410 ± 9	0.7 ± 0.1	
	1 month	454 ± 16	0.8 ± 0.1		-	-	

3.3. Cellular Experiments

To investigate the effect of Lips-C18Edv formulations on the inhibition of oxidative stress induced-cell death, a standardized *in vitro* cell model was used [34][4]. Based on our previous studies on ARPE19 cells [4], we selected 50 and 100 μM of C18Edv concentrations which did not induce any decrease in cellular viability after 48 h of treatment. The ability of Lips-C18Edv-10% and Lips-C18Edv-20% to protect retinal cells from oxidative stress induced-cell death was compared with that of free C18Edv and the results showed in **Figure 4A**. Because of its high colloidal instability, Lips-C18Edv-40% was not considered. The treatment with both liposomal formulations significatively increased cell survival with respect AAPH-treated cells although with different efficacy. At 50 and 100 μM antioxidant concentration, Lips-C18Edv-20% provided a cellular protection of about 15%

and 20% higher with respect to Lips-C18Edv-10%. No significative differences were observed between the effects of free C18Edv and Lips-C18Edv-10% formulation, while Lips-C18Edv-20% increased the efficacy of the bioactive molecule at the lowest concentration tested (20% more cell viability than free C18Edv, $p < 0.001$). The cellular protection provided by both free C18Edv and Lips-C18Edv-20% at 100 µM did not show significative differences but it is important to underlying that the lipophilic nature of C18Edv makes its a poorly water-soluble drug that cannot be administered without a delivery system. The different behaviour of these C18Edv liposomal formulations could be ascribed to the decrease of membrane fluidity observed in both MD and fluorescence experiments when it goes from the 10% to 20% of Edaravone in the formulations. It is well acknowledged that cellular uptake is affected by membrane fluidity [35] and more rigid nanoparticles can more easily enter the cells. In fact MD experiments showed [36] that fluid and flexible NP are subjected to deformation during the internalization and consequently the process requires more elastic deformation energy respect to rigid NP internalization that can be easily fully enveloped by the cell membrane. To confirm this hypothesis, cellular uptake studies by using calcein probe in flow cytometry analyses were performed: as shown in **Figure 4B-C**, Lips-C18Edv-20% were internalized more efficiently with respect to empty Lips and Lips-C18Edv-10% (22% and 14% more with respect free calcein-treated cells, respectively).

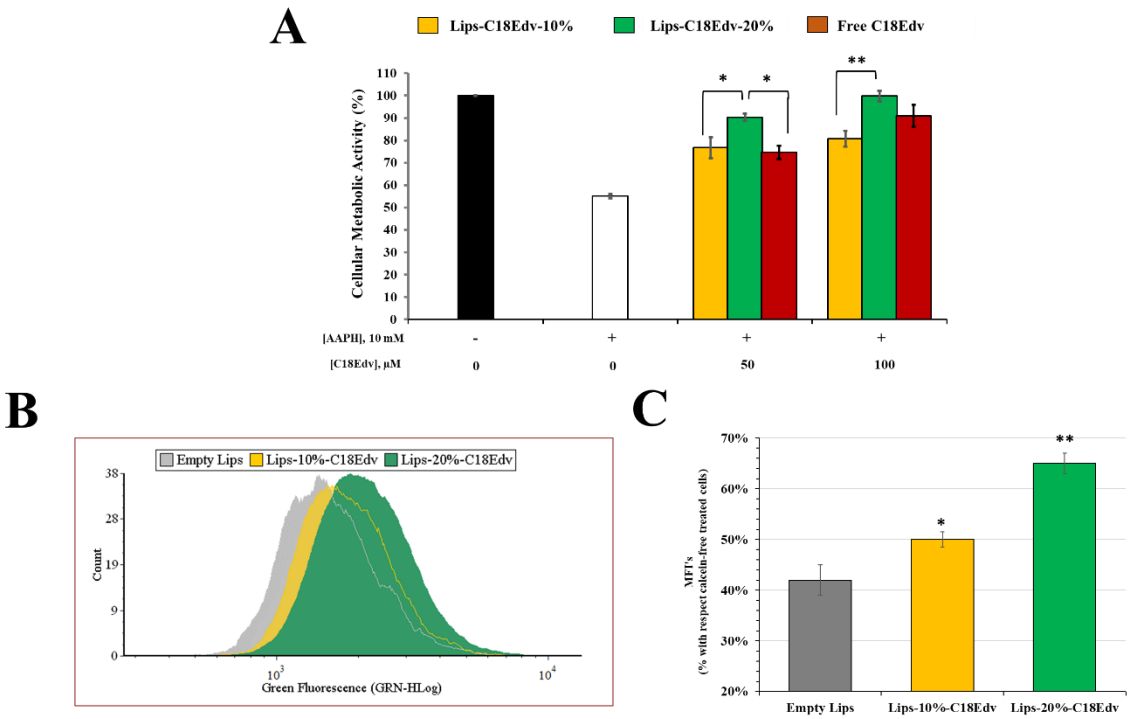

Figure 4. (A) Effect of free C18Edv and C18Edv incorporated in liposomes in ARPE19 cells after AAPH exposure by MTT assay. The cells were pre-treated with 50 and 100 µM free C18Edv or Lips-C18Edv-10% and Lips-C18Edv-20%, which correspond to 180 and 90 µg mL^{-1} lipid for 24 h, before being exposed to 10 mM AAPH for 24 h. **(B-C)** Cellular uptake studies performed using Empty Lips, Lips-C18Edv-10% and Lips-C18Edv-20% at final 90 µg mL^{-1} lipid concentration after 4 h of incubation. Data are expressed as means ± S.D. of five independent experiments, each performed in triplicate. *p<0.05 and **p<0.001.

Conclusion

In this work the lipophilic C18Edv has been introduced in a POPC liposomal bilayer and its influence on the liposome physical state, hydration and cellular activity has been studied by a combined computational-experimental approach. MD, fluorescence spectroscopy and DLS experiments showed that the presence of C18Edv increases liposome rigidity and conditions vesicles size and stability. The study highlights the fact that adjusting C18Edv percentage at a 20% w/w respect to POPC cellular uptake and antioxidant activity result maximized.

References

[1] S. Reuter, S.C. Gupta, M.M. Chaturvedi, B.B. Aggarwal, Oxidative stress, inflammation, and cancer: How are they linked?, Free Radic. Biol. Med. 49 (2010) 1603–1616. https://doi.org/10.1016/j.freeradbiomed.2010.09.006.

[2] I. Liguori, G. Russo, F. Curcio, G. Bulli, L. Aran, D. Della-Morte, G. Gargiulo, G. Testa, F. Cacciatore, D. Bonaduce, P. Abete, Oxidative stress, aging, and diseases, Clin. Interv. Aging. 13 (2018) 757–772. https://doi.org/10.2147/CIA.S158513.

[3] K. Kikuchi, N. Takeshige, N. Miura, Y. Morimoto, T. Ito, S. Tancharoen, K. Miyata, C. Kikuchi, N. Iida, H. Uchikado, N. Miyagi, N. Shiomi, T. Kuramoto, I. Maruyama, M. Morioka, K.I. Kawahara, Beyond free radical scavenging: Beneficial effects of edaravone (Radicut) in various diseases (Review), Exp. Ther. Med. 3 (2012) 3–8. https://doi.org/10.3892/etm.2011.352.

[4] C. Minnelli, E. Laudadio, R. Galeazzi, D. Rusciano, T. Armeni, P. Stipa, M. Cantarini, G. Mobbili, Synthesis, characterization and antioxidant properties of a new lipophilic derivative of edaravone, Antioxidants. 8 (2019). https://doi.org/10.3390/antiox8080258.

[5] S. Jo, T. Kim, V.G. Iyer, W. Im, CHARMM-GUI: A web-based graphical user interface for CHARMM, J. Comput. Chem. 29 (2008) 1859–1865. https://doi.org/10.1002/jcc.20945.

[6] D.Y. Villanueva, J.B. Lim, J.B. Klauda, Influence of ester-modified lipids on bilayer structure, Langmuir. 29 (2013) 14196–14203. https://doi.org/10.1021/la403919h.

[7] J.B. Klauda, B.R. Brooks, R.W. Pastor, Dynamical motions of lipids and a finite size effect in simulations of bilayers, J. Chem. Phys. 125 (2006). https://doi.org/10.1063/1.2354486.

[8] W.L. Jorgensen, J. Chandrasekhar, J.D. Madura, R.W. Impey, M.L. Klein, Comparison of simple potential functions for simulating liquid water, J. Chem. Phys. 79 (1983) 926–935. https://doi.org/10.1063/1.445869.

[9] A.P. Ruymgaart, R. Elber. Revisiting Molecular Dynamics on a CPU/GPU system: Water Kernel and SHAKE Parallelization. J Chem Theory Comput. 13 (2012) 4624-4636 doi:10.1021/ct300324k

[10] M.J. Abraham, T. Murtola, R. Schulz, S. Páll, J.C. Smith, B. Hess, E. Lindah, Gromacs: High performance molecular simulations through multi-level parallelism from laptops to supercomputers, SoftwareX. 1–2 (2015) 19–25. https://doi.org/10.1016/j.softx.2015.06.001.

[11] L. Serrano Cardona, E. Muñoz Mata, Paraninfo Digital, Early Hum. Dev. 83 (2013) 1–11.

https://doi.org/10.1016/j.earlhumdev.2006.05.022.

[12] C. Lee, W. Yang, R.G. Parr, Development of the Colle-Salvetti correlation-energy formula into a functional of the electron density, Phys. Rev. B. 37 (1988) 785–789. https://doi.org/10.1103/PhysRevB.37.785.

[13] P.J. Stephens, F.J. Devlin, C.F. Chabalowski, M.J. Frisch, Ab Initio calculation of vibrational absorption and circular dichroism spectra using density functional force fields, J. Phys. Chem. 98 (1994) 11623–11627. https://doi.org/10.1021/j100096a001.

[14] A.D. Becke, Density-functional thermochemistry. III. The role of exact exchange, J. Chem. Phys. 98 (1993) 5648–5652. https://doi.org/10.1063/1.464913.

[15] J.B. Klauda, R.M. Venable, J.A. Freites, J.W. O'Connor, D.J. Tobias, C. Mondragon-Ramirez, I. Vorobyov, A.D. MacKerell, R.W. Pastor, Update of the CHARMM All-Atom Additive Force Field for Lipids: Validation on Six Lipid Types, J. Phys. Chem. B. (2010). https://doi.org/10.1021/jp101759q.

[16] T. Darden, D. York, L. Pedersen, Particle mesh Ewald: An N·log(N) method for Ewald sums in large systems, J. Chem. Phys. 98 (1993) 10089–10092. https://doi.org/10.1063/1.464397.

[17] R.W. Hockney, J.W. Eastwood, Computer Simulation Using Particles, 1988. https://doi.org/10.1887/0852743920.

[18] J.W. Eastwood, R.W. Hockney, D.N. Lawrence, P3M3DP-The three-dimensional periodic particle-particle/ particle-mesh program, Comput. Phys. Commun. 19 (1980) 215–261. https://doi.org/10.1016/0010-4655(80)90052-1.

[19] E. Laudadio, R. Galeazzi, G. Mobbili, C. Minnelli, A. Barbon, M. Bortolus, P. Stipa, Depth Distribution of Spin-Labeled Liponitroxides within Lipid Bilayers: A Combined EPR and Molecular Dynamics Approach, ACS Omega. 4 (2019) 5029–5037. https://doi.org/10.1021/acsomega.8b03395.

[20] R.D. Porasso, J.J. López Cascales, A criterion to identify the equilibration time in lipid bilayer simulations, Pap. Phys. 4 (2012). https://doi.org/10.4279/PIP.040005.

[21] R. Zhang, C. Gao, S. Pan, R. Shang, Fusion of GNSS and speedometer based on VMD and its application in bridge deformation monitoring, Sensors (Switzerland). 20 (2020). https://doi.org/10.3390/s20030694.

[22] E.F. Pettersen, T.D. Goddard, C.C. Huang, G.S. Couch, D.M. Greenblatt, E.C. Meng, T.E. Ferrin, UCSF Chimera - A visualization system for exploratory research and analysis, J. Comput. Chem. 25 (2004) 1605–1612. https://doi.org/10.1002/jcc.20084.

[23] L.A. Bagatolli, Laurdan Fluorescence Properties in Membranes: A Journey from the Fluorometer to the Microscope. In: Mely Y, Duportail G (eds) Fluorescent methods to study biological membranes. Springer, Heidelberg/New York, 2013, pp 3–36

[24] T. Parasassi, M. Loiero, M. Raimondi, G. Ravagnan, E. Gratton, Absence of lipid gel-phase domains in seven mammalian cell lines and in four primary cell types, BBA - Biomembr. 1153 (1993) 143–154. https://doi.org/10.1016/0005-2736(93)90399-K.

[25] C. Minnelli, L. Cianfruglia, E. Laudadio, R. Galeazzi, M. Pisani, E. Crucianelli, D. Bizzaro, T. Armeni, G. Mobbili, Selective induction of apoptosis in MCF7 cancer-cell by targeted liposomes functionalised with mannose-6-phosphate, J. Drug Target. 26 (2018) 242–251. https://doi.org/10.1080/1061186X.2017.1365873.

[26] N. Kučerka, M.P. Nieh, J. Katsaras, Fluid phase lipid areas and bilayer thicknesses of

commonly used phosphatidylcholines as a function of temperature, Biochim. Biophys. Acta - Biomembr. 1808 (2011) 2761–2771. https://doi.org/10.1016/j.bbamem.2011.07.022.

[27] B.R. Lentz, Membrane “fluidity” as detected by diphenylhexatriene probes, Chem. Phys. Lipids. 50 (1989) 171–190. https://doi.org/10.1016/0009-3084(89)90049-2.

[28] S.S. Antollini, F.J. Barrantes, Disclosure of discrete sites for phospholipid and sterols at the protein - Lipid interface in native acetylcholine receptor-rich membrane, Biochemistry. 37 (1998) 16653–16662. https://doi.org/10.1021/bi9808215.

[29] L.A. Bagatolli, S.A. Sanchez, T. Hazlett, E. Gratton, Giant vesicles, laurdan, and two-photon fluorescence microscopy: Evidence of lipid lateral separation in bilayers, Methods Enzymol. 360 (2003) 481–500. https://doi.org/10.1016/S0076-6879(03)60124-2.

[30] T. Parasassi, G. De Stasio, G. Ravagnan, R.M. Rusch, E. Gratton, Quantitation of lipid phases in phospholipid vesicles by the generalized polarization of Laurdan fluorescence, Biophys. J. 60 (1991) 179–189. https://doi.org/10.1016/S0006-3495(91)82041-0.

[31] T. Parasassi, E.K. Krasnowska, L. Bagatolli, E. Gratton, Laurdan and Prodan as Polarity-Sensitive Fluorescent Membrane Probes, J. Fluoresc. 8 (1998) 365–373. https://doi.org/10.1023/A:1020528716621.

[32] M.P. Monopoli, C. Åberg, A. Salvati, K.A. Dawson, Biomolecular coronas provide the biological identity of nanosized materials, Nat. Nanotechnol. 7 (2012) 779–786. https://doi.org/10.1038/nnano.2012.207.

[33] S. Tenzer, D. Docter, J. Kuharev, A. Musyanovych, V. Fetz, R. Hecht, F. Schlenk, D. Fischer, K. Kiouptsi, C. Reinhardt, K. Landfester, H. Schild, M. Maskos, S.K. Knauer, R.H. Stauber, Rapid formation of plasma protein corona critically affects nanoparticle pathophysiology, Nat. Nanotechnol. 8 (2013) 772–781. https://doi.org/10.1038/nnano.2013.181.

[34] C. Minnelli, R. Galeazzi, E. Laudadio, A. Amici, D. Rusciano, T. Armeni, M. Cantarini, P. Stipa, G. Mobbili, Monoalkylated epigallocatechin-3-gallate (C18-EGCG) as novel lipophilic EGCG derivative: Characterization and antioxidant evaluation, Antioxidants. 9 (2020). https://doi.org/10.3390/antiox9030208.

[35] M.A. Bellavance, M.B. Poirier, D. Fortin, Uptake and intracellular release kinetics of liposome formulations in glioma cells, Int. J. Pharm. 395 (2010) 251–259. https://doi.org/10.1016/j.ijpharm.2010.05.017.

[36] J. Sun, L. Zhang, J. Wang, Q. Feng, D. Liu, Q. Yin, D. Xu, Y. Wei, B. Ding, X. Shi, X. Jiang, Tunable rigidity of (polymeric core)-(lipid shell) nanoparticles for regulated cellular uptake, Adv. Mater. 27 (2015) 1402–1407. https://doi.org/10.1002/adma.201404788.